Self-consistency and universality of camera lens distortion models

Zhongwei Tang, Rafael Grompone von Gioi, Pascal Monasse, Jean-Michel Morel

Self-consistency and universality of camera distortion models

Zhongwei Tang,[1,*] Rafael Grompone von Gioi,[2] Pascal Monasse,[3] and Jean-Michel Morel[2]
[1] ECE, Duke University, Durham, USA
[2] CMLA, ENS-Cachan, Cachan, France
[3] IMAGINE, LIGM, Université Paris-Est/École des Ponts ParisTech, France
[*] Corresponding author: tang@cmla.ens-cachan.fr

***Abstract*—This paper introduces the concepts of "self-consistency" and "universality" to evaluate high precision camera distortion models. Self-consistency is evaluated by the residual error when the distortion generated with a certain model is corrected by the best parameters for the same model (used in reverse way, which is common practice). Analogously, universality is measured by the residual error when a model is used to correct distortions generated by a family of other models. Five classic camera distortion models are reviewed and compared for their degree of self-consistency and universality. Among the evaluated models, it is concluded that only the polynomial and the rational models are universal up to precisions of 1/100 pixel. However, the polynomial model, being linear, is much simpler and faster to estimate. Unusually high polynomial degrees are required to reach this strong precision. Nevertheless, extensive numerical experiments show that such distortion polynomials are easily estimated and produce a precise distortion correction without over-fitting. Our conclusions are validated by three independent experimental setups: The models are compared first in synthetic experiments by their approximation power; second by fitting a real camera distortion estimated by a non parametric algorithm; and finally by the absolute correction measurement provided by photographs of tightly stretched strings, warranting a high straightness.**

I. Introduction

The pinhole camera model is widely used in computer vision applications because of its simplicity and its linearity in terms of projective geometry [14]. But real cameras deviate from the ideal pinhole model, mainly because of lens geometric distortion [2], and possibly from the CCD shape distortion itself. Thus an accurate camera distortion correction is the first step towards high precision 3D metric reconstruction from photographs. With the steady progress in lens quality and computing power, high-precision 3D reconstructions become feasible, demanding in turn higher camera distortion precisions than those provided by classic methods. The object of this paper is to investigate the validity of distortion models at the light of precision requirements increased by two to three orders of magnitude. This increased accuracy requires a new methodology for evaluating distortion models. In a nutshell, our conclusion is that a polynomial model of higher degree than usual, ranging from 8 to 15, is necessary for reaching a pixel precision ranging from $1/100$ to $1/1000$. The polynomial model permits to approximate at this resolution any other model, and the inverse of any other model, including itself. When these properties are reached, the model is called *universal* and *self-consistent*. Among the other four models which will be compared (radial, division, FOV, and rational), only the rational model has the eligible self-consistency and universality, but to a far higher computational cost.

With the exception of a few non-parametric methods [8], [25], [12], an appropriate distortion model is indispensable to model the deviation of a real camera from an ideal pinhole camera. The main distortion models are the radial model [2], the division model [9], the FOV model [7], the bicubic model [15], the rational model [5], [13]. This diversity is only marginally linked to the kind of camera. Thus, a synthetic quantitative and qualitative comparison is required. Do these models reflect camera distortion in its physical aspect? It could be argued that a correct model should originate from physical measurements on systems of lenses. Surprisingly enough, there is little physical background for the distortion models in the literature. In [29], lens distortion is decomposed into three effects: radial distortion, decentering distortion and thin prism distortion. But, still, it is only marginally based on a physical background. In fact, the final distortion includes effects caused by a complex lens system, by the camera geometry, and by the (not perfectly planar) shape of the captor. One is therefore led to figure out a flexible model with enough parameters to approximate any plausible distortion. In absence of a physical model, the model classification approach adopted here will be to look for models which actually cope with any other proposed distortion model, at a given precision.

The second question is the relationship between the distortion and the correction models, which should be inverse of each other. A distortion model is used to simulate the distortion of ideal images, while a correction model is used to correct distorted images. Indeed, most of the widely used models are not invertible, thus the *correction model* and the *distortion model* must be different. In the literature, however, it seems that the roles of *distorted point* and *undistorted point* are interchangeable, which again confirms the lack of physical meaning for these models. For example, direct distortion models are used in global camera calibration [28], [31], [17], [29]. Yet, in most plumb-line methods [2], [7], [1], [20], [23], [22], [4] or some pattern-free methods [24], [30], [9], [18], [27], [5], [21], [3], [16], the very same correction models are used without any fuss to approximate the inverse distortion.

Assume we simulate a camera distortion with a certain model and a certain set of parameters. Except for some models,

the distortion will not be corrected by using the same model with other parameters, because the model itself is usually not *invertible*. We propose to measure the error incurring when a distortion is inverted by using the same model as the one used for simulating the distortion. This inversion error, when the best correcting parameters have been estimated and applied, will be a measurement of the model *self-consistency*. In other words, self-consistency relates to how well a model is able to correct distortion generated by a model of its own family. Of course the best models should be universal, therefore able to correct distortions generated by other models. We therefore propose to measure a model *universality* as the residual error when this model is used to correct distortion generated by a whole set of different models. A *universal model* is a model for which this error is very small no matter what other (reasonable) distortion model has been applied. A self-consistent and universal model implies that the model can also approximate the distortion generated by other models. Our goal is to identify the least complex universal and self-consistent models. Of course this question only makes sense within fixed accuracy bounds. None of the classic models is actually exactly (algebraically) invertible. Thus, the introduced concepts, universality and self-consistency, must be thought of with the *to a given precision* caveat. As a matter of fact, for off-the-shelf cameras, most distortion models are roughly equivalent at a 1 pixel precision. The question is different when we aim at sub-pixel precisions. These precisions, up to 1/100 pixel, are highly desirable when using cameras for stereovision or photogrammetric tasks.

The other caveat is that, although distortion models reflect a model of the optical lens, the real corrected distortion must actually involve the whole system lens + CCD. There is no way to guarantee that a CCD is absolutely flat, or exactly perpendicular to the optical axis. This explains why the camera distortion modeling remains, after all, an empirical question where no physical argument can be final. The ultimate decision is numerical.

The various distortion models will be carefully compared on realistic synthetic distortion data permitting to quantify the ideal attainable precision. Then, the same models will be compared on their capacity to fit a real camera distortion (estimated by a non-parametric algorithm [12]). Finally, the distortion correction accuracy by each model will be evaluated by using the plumb-line approach, with photographs of tightly stretched strings, warranting a high straightness, and giving absolute measurements of the correction quality [26]. In short, there will be three different numerical validations of our conclusions.

This paper is organized as follows. Section II reviews five classic distortion models. Their self-consistency and universality are evaluated in Section III by synthetic experiments. Section IV and V describe the experiments done with real cameras. Section VI is a conclusion.

II. Distortion and Correction models

Let us denote by (x_u, y_u) the coordinates of an undistorted point as would be observed in an ideal pinhole camera. Due to the lens geometric distortion, this point will be distorted to coordinates (x_d, y_d). We will model distortion by a function f that transforms undistorted to distorted coordinates,

$$\begin{aligned} x_d &= f_x(x_u, y_u), \\ y_d &= f_y(x_u, y_u). \end{aligned} \tag{1}$$

A correction model g performs the transformation in the opposite direction:

$$\begin{aligned} x_u &= g_x(x_d, y_d), \\ y_u &= g_y(x_d, y_d). \end{aligned} \tag{2}$$

A particularly interesting case is when the functions f or g show radial symmetry relative to a fixed distortion center (x_c, y_c). In that case we obtain a compact formulation using normalized coordinates $\bar{x}_u = x_u - x_c$, $\bar{y}_u = y_u - y_c$, $\bar{x}_d = x_d - x_c$ and $\bar{y}_d = y_d - y_c$; then, the distortion can be expressed as the transformation of the undistorted radius $r_u = \sqrt{\bar{x}_u^2 + \bar{y}_u^2}$ to the distorted radius $r_d = \sqrt{\bar{x}_d^2 + \bar{y}_d^2}$.

We start by reviewing the most current models, namely the radial model [2], the division model [9], the FOV model [7], the polynomial model [15], and the rational function model [5], [13]. We will write the models as transforming from coordinates (x_1, y_1) to (x_2, y_2). When a model would be used as a distortion model, (x_1, y_1) will correspond to (x_u, y_u) and (x_2, y_2) to (x_d, y_d), and it is the opposite when used as a correction model.

The radial model displaces a point along its radial direction originating at the distortion center. The distorted new radius r_2 is a function of the original radius r_1,

$$r_2 = r_1(k_0 + k_1 r_1 + k_2 r_1^2 + \cdots). \tag{3}$$

The parameter k_0 representing a scaling does not introduce distortion. The scaled image is distorted by $k_1, k_2, \ldots$. If $k_1, k_2, \ldots$ are all positive, we have a *pincushion distortion*; if $k_1, k_2, \ldots$ are all negative, a *barrel distortion*. *Mustache distortion* occurs if the signs of $k_1, k_2, \ldots$ are not the same. Note that the distortion center (x_c, y_c) is also a parameter of radial models.

The *division model* is nothing but the scalar inverse of the radial model,

$$r_2 = \frac{r_1}{k_0 + k_1 r_1 + k_2 r_1^2 + \cdots}. \tag{4}$$

In these models, high-order coefficients are needed to model extreme distortion in fish-eye lenses or other wide angle lens systems. A more sparse representation is obtained by parameterizing the distortion by the field of view (FOV). The only parameter of the FOV model is the field of view ω:

$$r_2 = r_1 \frac{\tan(r_1 \omega)}{2 r_1 \tan(\frac{\omega}{2})}. \tag{5}$$

Here the coefficient ω is of order 1, but more coefficients can be added to the FOV model to make it more complete.

In the *polynomial model* the distortion is modeled as a polynomial in x_1 and y_1. For example, the third order (bicubic)

polynomial model is

$$\begin{aligned} x_2 &= a_1x_1^3 + a_2x_1^2y_1 + a_3x_1y_1^2 + a_4y_1^3 + a_5x_1^2 \\ &\quad + a_6x_1y_1 + a_7y_1^2 + a_8x_1 + a_9y_1 + a_{10}, \\ y_2 &= b_1x_1^3 + b_2x_1^2y_1 + b_3x_1y_1^2 + b_4y_1^3 + b_5x_1^2 \\ &\quad + b_6x_1y_1 + b_7y_1^2 + b_8x_1 + b_9y_1 + b_{10}. \end{aligned} \quad (6)$$

The rational function model is a quotient of two polynomials. A second order rational function model can be written as

$$\begin{aligned} x_2 &= \frac{a_1x_1^2 + a_2x_1y_1 + \cdots + a_5y_1 + a_6}{c_1x_1^2 + c_2x_1y_1 + \cdots + c_5y_1 + c_6}, \\ y_2 &= \frac{b_1x_1^2 + b_2x_1y_1 + \cdots + b_5y_1 + b_6}{c_1x_1^2 + c_2x_1y_1 + \cdots + c_5y_1 + c_6}. \end{aligned} \quad (7)$$

III. Self-consistency and Universality

In the literature it is not always clear whether the above models are correction models or distortion models. This raises the question of *self-consistency*, while the *universality* question is raised by the plurality of models. Being theoretical properties of model families, both properties can be genuinely evaluated by synthetic experiments. Self-consistency and universality will be tested by generating a distortion with any of the above models, and then evaluating the residual error after applying the best distortion correction with each model. Of course, we will use for each model sets of parameters that generate a realistic distortion, as illustrated in Table I. A distortion is generated using a first model in direct way, using Eq. (1). This distortion is then corrected by identifying the best parameters of a second model when used as in Eq. (2).

In our synthetic tests, both (x_u, y_u) and (x_d, y_d) are known. The question is how well the ideal points (x_u, y_u) can be approached by $g_x(x_d, y_d)$ and $g_y(x_d, y_d)$. We want to compute the coefficients of g_x and g_y by minimizing the difference between the ideal correction and the practical correction. The energy to be minimized can be written as

$$\begin{aligned} C &= \int\int \big(g_x(x_d, y_d) - x_u\big)^2 \\ &\quad + \big(g_y(x_d, y_d) - y_u\big)^2 \mathrm{d}x_d \mathrm{d}y_d. \end{aligned} \quad (8)$$

In practice, the simulation is performed on M samples $(x_{u_i}, y_{u_i}), i = 1, \ldots, M$ regularly distributed on an image. The corresponding distorted samples $(x_{d_i}, y_{d_i}), i = 1, \ldots, M$ are obtained by Eq (1). The discrete energy to be minimized is

$$D = \sum_{i=1}^{M} \big(g_x(x_{d_i}, y_{d_i}) - x_{u_i}\big)^2 + \big(g_y(x_{d_i}, y_{d_i}) - y_{u_i}\big)^2. \quad (9)$$

Given the two coordinates for each of the M points, we have $2M$ equations relating the ideal and the distorted points. In the case of the polynomial model these equations have the form given in Eq. (6), and the problem can be formulated as a linear system

$$\mathbf{A}\mathbf{k} = \mathbf{b}, \quad (10)$$

where $\mathbf{A}$ is a matrix containing the different powers for all the distorted points, $\mathbf{k}$ is formed with the model's coefficients, and $\mathbf{b}$ contains the undistorted coordinates. The set of model coefficients with least error D is obtained by minimizing the norm $\|\mathbf{A}\mathbf{k} - \mathbf{b}\|_2$, which results in

$$\mathbf{k} = \left(\mathbf{A}^T\mathbf{A}\right)^{-1}\mathbf{A}^T\mathbf{b}. \quad (11)$$

In practice, the matrix $\mathbf{A}$ is ill-conditioned and can make the solution unstable. Some normalization technique should be applied before.

The same linear method can be applied to the radial model when the distortion center is known because the transformation Eq. (3) is also linear.[1] For all the other models, a non-linear method must be used, even if (x_c, y_c) is known. The minimization is performed by first doing an incremental Levenberg-Marquardt (LM) algorithm which estimates the parameters in increasing order. The algorithm starts estimating the parameters of a low order model; the result is used to initialize the model with the next higher order, and the process continues until the aimed order. The Jacobian matrix $\mathbf{J}$ required by LM is computed explicitly to make the algorithm efficient. Even though this strategy is complex, it avoids some local minima and is safer than performing LM directly on the model of the aimed order.

A. Experiments with known distortion center

For our first experiment, a total of $M = 5104$ points were regularly distributed in an image domain of size 1761×1174 and the distortion center was fixed at $(880.5, 587)$ and was assumed to be known. The corresponding distorted points were computed using the different models with the parameters in Table I. The self-consistency and universality measurements are recapitulated in Table II, expressed as the average error $\bar{D} = \sqrt{\frac{D}{M}}$ after estimating the parameters which minimize the energy in Eq (9).

B. Experiments with unknown distortion center

In practice, the distortion center (x_c, y_c) is unknown and it should also be considered as a parameter in the minimization formulation. Our second experiment was done in this way. The minimization problem becomes now non-linear for most models. This is true for the radial model, the division model and the FOV model. In contrast, the polynomial and the rational function models are invariant to a translation of the distortion center. The point (x_c, y_c) can be fixed arbitrarily, and in the polynomial case the minimization problem is still linear. This is a decisive advantage with respect to the other models. The self-consistency and universality results are recapitulated in Table III with the same parameters for generating distortion in Table I. For the distortion generation, the distortion center was fixed again at the center $(880.5, 587)$ of the image, while for the correction the initial distortion center was realistically taken $(50, 50)$ pixels away from the true position. For the radial model and the division model, the Levenberg-Marquardt algorithm could still find the true distortion center, and the

[1] According to [4], the rational function model can also be solved linearly by minimizing some algebraic error. But this error is not directly related to the geometric error we want to minimize and sometimes leads to undesirable result.

model	parameters
radial 2° $1084 \rightarrow 1050$	$k_0 = 1.0$, $k_1 = 0.25 \times 10^{-4}$, $k_2 = -0.5 \times 10^{-7}$
radial 4° $991.6 \rightarrow 1050$	$k_0 = 1.0$, $k_1 = 0.25 \times 10^{-4}$, $k_2 = -0.5 \times 10^{-7}$, $k_3 = 1.0 \times 10^{-10}$, $k_4 = -1.5 \times 10^{-14}$
division 2° $1083 \rightarrow 1050$	$d_0 = 1.0$, $d_1 = -0.25 \times 10^{-4}$, $d_2 = 0.5 \times 10^{-7}$
division 4° $988.7 \rightarrow 1050$	$d_0 = 1.0$, $d_1 = -0.25 \times 10^{-4}$, $d_2 = 0.5 \times 10^{-7}$, $d_3 = -1.0 \times 10^{-10}$, $d_4 = 1.5 \times 10^{-14}$
FOV 3° $501.4 \rightarrow 1050$	$k_0 = 1.0$, $\omega = 1.0 \times 10^{-3}$, $k_2 = -2.0 \times 10^{-7}$, $k_3 = 4.0 \times 10^{-10}$
polynomial 3° $1050 \rightarrow 1064$	$a_1 = b_1 = -1.0 \times 10^{-8}$, ..., $a_5 = b_5 = 2.0 \times 10^{-5}$, ..., $a_8 = 0.9$, $a_9 = 0.1$, $a_{10} = 0.0$, $b_8 = 0.1$, $b_9 = 0.9$, $b_{10} = 0.0$
polynomial 4° $1050 \rightarrow 1075$	$a_1 = b_1 = 5.0 \times 10^{-12}$, $a_6 = b_6 = -1.0 \times 10^{-8}$, $a_{10} = b_{10} = 2.0 \times 10^{-5}$, ..., $a_{13} = 0.9$, $a_{14} = 0.1$, $a_{15} = 0.0$, $b_{13} = 0.1$, $b_{14} = 0.9$, $b_{15} = 0.0$
rational 2° $1031 \rightarrow 1104$	$a_1 = 1.0 \times 10^{-5}$, $a_2 = 2.0 \times 10^{-5}$, $a_3 = 3.0 \times 10^{-5}$, $a_4 = 0.9$, $a_5 = 0.1$, $a_6 = 0.0$ $b_1 = 3.0 \times 10^{-5}$, $b_2 = 2.0 \times 10^{-5}$, $b_3 = 1.0 \times 10^{-5}$, $b_4 = 0.1$, $b_5 = 0.9$, $b_6 = 0.0$ $c_1 = 1.0 \times 10^{-8}$, $c_2 = 1.0 \times 10^{-8}$, $c_3 = 1.0 \times 10^{-8}$, $c_4 = 0.0001$, $c_5 = 0.0001$, $c_6 = 1.0$

TABLE I

MODELS USED TO GENERATE DISTORTION, WITH THEIR REALISTIC PARAMETERS. THE VALUES ON THE LEFT AND ON THE RIGHT OF THE SIGN "$\rightarrow$" ARE THE UNDISTORTED RADIUS AND THE DISTORTED RADIUS RESPECTIVELY. FOR THE POLYNOMIAL MODEL, THE COEFFICIENTS ARE THE SAME FOR x AND y COMPONENT, EXCEPT FOR THE ORDER 1 COEFFICIENTS. NOTE THAT THE DISTORTION CAN BE BARREL, PINCUSHION OR MUSTACHE.

		Distortion Generation Model							
		R 2°	R 4°	D 2°	D 4°	F 3°	P 3°	P 4°	Ra 2°
Correction Model	R 2°	0.09	0.1	0.06	0.2	0.03	60	60	70
	R 4°	**0.002**	**0.002**	**0.0008**	**0.002**	**0.0008**	60	60	70
	D 2°	0.06	0.2	0.03	0.2	0.04	60	60	70
	D 4°	**0.001**	**0.001**	**0.0004**	**0.001**	**0.0007**	60	60	70
	F 3°	0.08	0.07	0.09	0.06	0.02	60	60	70
	P 3°	0.6	0.5	0.5	0.6	0.2	0.2	0.7	0.5
	P 4°	0.6	0.5	0.5	0.6	0.2	0.05	0.1	0.07
	P 8°	0.06	0.02	0.06	0.02	**0.007**	**0.00007**	**0.0007**	**0.00004**
	P 15°	**0.01**	**0.008**	**0.01**	**0.008**	**0.0003**	**0.0000001**	**0.0000002**	**0.0000004**
	Ra2°	5	7	5	7	40	0.5	0.4	0.1
	Ra6°	0.05	0.03	0.1	0.09	0.1	**0.000002**	**0.0001**	**0.00000008**
	Ra14°	**0.01**	**0.009**	**0.01**	**0.01**	**0.009**	**0.00000003**	**0.000002**	**0.0000000002**

TABLE II

SELF-CONSISTENCY AND UNIVERSALITY WITH KNOWN DISTORTION CENTER. THE AVERAGE ERROR ($\bar{D}$) (IN PIXELS) IS SHOWN. THE LEFT COLUMN ENTRIES SHOW THE MODEL AND THE ORDER USED FOR CORRECTION. THE TOP ENTRY ROW GIVES THE MODEL AND THE ORDER USED TO GENERATE THE DISTORTION. THE FIVE COMPARED MODEL CLASSES ARE R-RADIAL, D-DIVISION, F-FOV, P-POLYNOMIAL, AND RA-RATIONAL. THE PARAMETERS IN TABLE I WERE USED TO GENERATE THE DISTORTION. THE BOLD FONT IS USED TO HIGHLIGHT THE AVERAGE ERROR $\bar{D} \leqslant 10^{-2}$.

minimized error was the same as when the distortion center was known. Nevertheless, for the FOV model, a wrong initialization of the distortion center degraded the correction performance. For the polynomial model, the solution can be found linearly by fixing an arbitrary distortion center.

C. Comparison

We aim at an average precision below 10^{-2} pixel. The tables show that the models are self-consistent if the order of correction is high enough. The radial model and the division model are consistent with each other, whether the distortion center is known or not. The FOV model is a little less consistent with the radial symmetric models, including itself, when the distortion center is known. With an unknown distortion center, the FOV correction performance decays. The polynomial model instead seems to be able to correct any type of distortion, but a higher order is often necessary to correct the radial, division or FOV distortions. This higher order is not a problem, because of the computational efficiency of the linear method. The rational model has a comparable performance at the price of a much higher computational cost. In conclusion, at precision $1/100$ pixels the polynomial and the rational models are the only ones to be jointly self-consistent, universal and linear among the compared models. But the polynomial model has a much lower complexity than the rational model to attain the same precision. A degree 8 polynomial model is enough to attain precisions strictly below $1/10$. The $1/100$ pixel precision is robustly attainable with degree 15 polynomials.

D. Realistic distortion

A real distortion can be far more complex than what the above simple models can generate. A more realistic distortion contains a radial symmetric term, a term for decentering distortion and a term for thin prism distortion [29],

$$\begin{aligned} \bar{x}_d &= \bar{x}_u \left(k_0 + k_1 r_u + k_2 r_u^2 + \cdots\right) \\ &\quad + \left[p_1 \left(r_u^2 + 2\bar{x}_u^2\right) + 2p_2 \bar{x}_u \bar{y}_u\right] \left(1 + p_3 r_u^2\right) + s_1 r_u^2, \\ \bar{y}_d &= \bar{y}_u \left(k_0 + k_1 r_u + k_2 r_u^2 + \cdots\right) \\ &\quad + \left[p_2 \left(r_u^2 + 2\bar{y}_u^2\right) + 2p_1 \bar{x}_u \bar{y}_u\right] \left(1 + p_3 r_u^2\right) + s_2 r_u^2, \end{aligned}$$

Correction Model \ Distortion Generation Model	R 2°	R 4°	D 2°	D 4°	F 3°	P 3°	P 4°	Ra 2°
R 2°	0.09	0.1	0.06	0.2	0.03	60	60	70
R 4°	**0.002**	**0.002**	**0.0008**	**0.002**	**0.0008**	60	60	70
D 2°	0.06	0.2	0.03	0.2	0.04	60	60	70
D 4°	**0.001**	**0.001**	**0.0004**	**0.001**	**0.0007**	60	60	70
F 3°	0.7	3	2	3	40	60	60	70
P 3°	0.6	0.5	0.5	0.6	0.2	0.2	0.7	0.5
P 4°	0.6	0.5	0.5	0.6	0.2	0.05	0.1	0.07
P 8°	0.06	0.02	0.06	0.02	**0.007**	**0.00007**	**0.0007**	**0.00004**
P 15°	**0.01**	**0.008**	**0.01**	**0.008**	**0.0003**	**0.0000001**	**0.0000002**	**0.0000004**
Ra2°	5	7	5	7	40	0.5	0.4	0.1
Ra6°	0.05	0.03	0.1	0.09	0.1	**0.000002**	**0.0001**	**0.00000008**
Ra14°	**0.01**	**0.009**	**0.01**	**0.01**	**0.009**	**0.00000003**	**0.000002**	**0.0000000002**

TABLE III

SELF-CONSISTENCY AND UNIVERSALITY WITH UNKNOWN DISTORTION CENTER. THE INITIAL DISTORTION CENTER WAS SET $(50, 50)$ PIXELS AWAY FROM ITS TRUE POSITION. THE AVERAGE ERROR ($\bar{D}$) (IN PIXELS) IS SHOWN. THE LEFT COLUMN ENTRIES GIVE THE MODEL AND THE ORDER USED FOR CORRECTION. THE TOP ROW ENTRIES GIVE THE MODEL AND THE ORDER USED TO GENERATE THE DISTORTION. THE FIVE COMPARED MODEL CLASSES ARE R-RADIAL, D-DIVISION, F-FOV, P-POLYNOMIAL, AND RA-RATIONAL. THE PARAMETERS IN TABLE I WERE USED TO GENERATE THE DISTORTION. THE BOLD FONT IS USED TO HIGHLIGHT THE AVERAGE ERROR $\bar{D} \leqslant 10^{-2}$.

with p_1, p_2, p_3 parameters for decentering distortion and s_1, s_2 parameters for thin prism distortion. They contribute to both radial symmetric distortion and tangential distortion. In Table IV, the self-consistency and universality of the models were again tested with known distortion center after adding the additional distortion with $p_1 = 4.0 \times 10^{-6}, p_2 = -2.0 \times 10^{-6}, p_3 = 0, s_1 = 3.0 \times 10^{-6}, s_2 = 1.0 \times 10^{-6}$. By adding a non-radial component in the distortion, the radial model, the division model and the FOV model do not reach anymore the 10^{-2} pixel precision. Both polynomial model and rational function model give a precision equal or better than 10^{-2} pixel with a high model order. But it is always linear to solve the parameters of polynomial model, while it requires a complex incremental LM minimization to solve rational function model.

IV. REAL DISTORTION FITTING EXPERIMENTS

After its validation on synthetic examples, we present here real tests to verify that the proposed high order polynomial model works for real distortion correction. This test is based on the non-parametric camera distortion estimation method in [12] but could be performed on any distortion model obtained by blind correction. This method requires a highly textured planar pattern, which is obtained by printing a textured image and pasting it on a very flat object (a mirror was used in the experiments). Two photos of the pattern were taken by a Canon EOS 30D SLR camera with EFS $18-55$mm lens. The minimal focal length (18mm) was chosen (with fixed focus) to produce a fairly large distortion. The distortion was estimated (up to a homography) as the diffeomorphism mapping the original digital pattern to a photograph of it. Without going into details, the algorithm is summarized in the following:

1) Take two slightly different photographs of a textured planar pattern with a camera whose settings are frozen;
2) apply the SIFT method [19] between the original digital pattern and both photographs to obtain matching pairs of points;
3) eliminate outliers by a loop validation step;
4) triangulate and interpolate the remaining matches to get a dense reverse distortion field;
5) refine the precision of the SIFT matching by correcting each matching point in one image with the local homography estimated from its neighboring matching points;
6) by applying the reverse distortion field to all images produced by the same camera, the camera is converted into a virtual pinhole camera.

The matching pairs delivered by step 5 (about 8000 in our experiments) in the above algorithm are "outliers"-free and precise thanks to the loop validation and filtering by local homography. So we can directly try all models to fit these "outliers"-free matchings. The residual fitting error shows to what extent the models are faithful to a real camera distortion. Under the assumption that the textured pattern is flat, the mapping from the digital pattern to the photo can be modeled classically as $\mathbf{S}\mathcal{D}\mathbf{H}$, with $\mathbf{H}$ the homography from the digital pattern to the photo, $\mathcal{D}$ the non-linear lens distortion and $\mathbf{S}$ a diagonal matrix to model the slant of the CCD matrix:

$$\mathbf{H} = \begin{pmatrix} h_{11} & h_{12} & h_{13} \\ h_{21} & h_{22} & h_{23} \\ h_{31} & h_{32} & 1 \end{pmatrix}, \quad \mathbf{S} = \begin{pmatrix} 1 & 0 & 0 \\ 0 & s & 0 \\ 0 & 0 & 1 \end{pmatrix}. \qquad (12)$$

Since the polynomial model and the rational function model can approximate well $\mathbf{H}$ and $\mathbf{S}$, we can use these models to approximate the distortion field without explicitly estimating the homography. Nevertheless, for the radial symmetric models, it is necessary to take into account $\mathbf{H}$ and $\mathbf{S}$ when approximating the distortion. Indeed $\mathbf{H}$ and $\mathbf{S}$ are generally not radial symmetric. Thus, we have 9 additional parameters to estimate, besides the parameters of radial symmetric distortion model. The polynomial model can again be solved linearly. For all the other models, an incremental LM minimization was used to estimate the distortion center, the distortion parameters and the homography.

Half of the matching pairs were used to estimate the parameters for the different models, and the other half to evaluate the average fitting error. The results are recapitulated in Table VI. They show that by combining $\mathbf{H}$ and $\mathbf{S}$ to model the inclination between the camera and the pattern, all of the radial symmetric models give almost the same fitting error, which becomes stable (0.15 pixel) when the order attains 4.

Correction Model \ Distortion Generation Model	R 2°	R 4°	D 2°	D 4°	F 3°	P 3°	P 4°	Ra 2°
R 2°	7	5	7	5	0.7	60	60	70
R 4°	7	5	7	5	0.7	60	60	70
D 2°	7	5	7	5	0.7	60	60	70
D 4°	7	5	7	5	0.7	60	60	70
F 3°	7	5	7	5	0.7	60	60	70
P 3°	0.6	0.5	0.5	0.6	0.2	0.3	0.8	0.3
P 4°	0.6	0.5	0.5	0.6	0.2	0.06	0.2	0.05
P 8°	0.06	0.02	0.06	0.02	**0.007**	**0.0001**	**0.001**	**0.00001**
P 15°	**0.01**	**0.008**	**0.01**	**0.008**	**0.0003**	**0.0000003**	**0.0000003**	**0.0000003**
Ra2°	5	7	5	7	40	0.8	0.5	0.1
Ra6°	0.05	0.03	0.1	0.09	0.1	**0.000006**	**0.005**	**0.00000007**
Ra14°	**0.01**	**0.009**	**0.01**	**0.01**	**0.009**	**0.00000005**	**0.000002**	**0.0000000001**

TABLE IV

SELF-CONSISTENCY AND UNIVERSALITY WITH KNOWN DISTORTION CENTER. ADDITIONAL DECENTERING AND THIN-PRISM DISTORTION IS ADDED. COMPARE WITH TABLES II AND III. EACH ENTRY SHOWS THE AVERAGE ERROR ($\bar{D}$) (IN PIXELS). THE PARAMETERS IN TABLE I WERE USED TO GENERATE THE DISTORTION. THE BOLD FONT IS USED TO HIGHLIGHT THE AVERAGE ERROR $\bar{D} \leqslant 10^{-2}$. THE ONLY NON-BOLD TO BOLD LINES ARE OBTAINED FOR THE POLYNOMIAL MODEL WITH DEGREE 8 TO 15.

Table V shows $\mathbf{H}$ and $\mathbf{S}$ estimated by three radial symmetric models of order 12. The similar estimation of $\mathbf{H}$ and $\mathbf{S}$ implies that the minimization process is stable.

The polynomial model and the rational function model give a stable fitting error (0.04 pixel), which is about 4 times smaller than the radial symmetric models. The stability of the fitting error confirms that none of the models suffers from numerical instability or noise fitting. We remark that the fitting error of the rational function model becomes stable when its order attains 4 (45 parameters to be estimated), while the polynomial model gives a stable fitting error when its order attains 7 (72 parameters to be estimated). Even though in this experiment the rational function model converges faster than the polynomial model, solving the rational function model requires a complex incremental LM minimization, which is a time-consuming process requiring a good initialization and does not always ensure the convergence to the global minimum,[2] while the polynomial model can always be solved linearly.

The fact that the polynomial model and the rational function model give fitting errors about 4 times smaller than the radial symmetric models implies that the real camera distortion is not strictly radial symmetric. Otherwise, the fitting error of the radial symmetric models should be at least as small as 0.04 pixel. The residual fitting error (0.04 pixel) given by the polynomial model and the rational function model can be attributed to the noise of matching points.

V. PLUMB-LINE VALIDATION

It should be noted that the non-parametric method does not give a ground truth. It is just a non-parametric estimation of the camera distortion, and it is subject to errors. Thus, we need a more objective evaluation to check the quality of the correction models. To this purpose, a physical frame with tightly stretched cylindrical strings was built [26]. The physical tension of the strings guarantees a very high straightness. Once the parameters of the models are estimated, a distortion field can be constructed and applied for the distortion correction of images of strings taken by the same camera with the same fixed lens configuration (see Fig. 1). The average distance from the edge points (computed by the method of [6]) of the corrected lines to the corresponding regression line was computed. See [26] for more details. Table VII recapitulates average distance for all lines in the image. According to Table VI, the stabilized fitting error implies that none of the models has the problem of noise fitting, which guarantees the correction quality and stability. The polynomial model gives a stable performance when the order attains 6, *which means that a polynomial model of order* 6 *was already capable of capturing the whole distortion.* The rational model gives a comparable performance when its order attains 4, at the price of more complex non-linear incremental minimization which does not ensure a global minimum. The residual straightness error of corrected lines is due to the fact that the mirror on which we pasted the pattern is not completely flat. All the radial symmetric models give a straightness error larger than the polynomial model and the rational function model, due to the flatness error of the pattern and to the non radial symmetric component in the camera distortion which the radial symmetric

[2]The linear solution to the rational function model proposed in [4] does not give a precise result in this case.

order	Radial	Division	FOV	Polynomial	Rational
3	0.29	0.29	0.28	1.48	0.19
4	0.15	0.15	0.15	1.26	0.05
5	0.15	0.15	0.15	0.21	0.05
6	0.15	0.15	0.15	0.08	0.05
7	0.15	0.15	0.15	0.04	0.04
8	0.15	0.15	0.15	0.04	0.04
9	0.15	0.15	0.15	0.04	0.04
10	0.15	0.15	0.15	0.04	0.04
11	0.15	0.15	0.15	0.04	0.04
12	0.15	0.15	0.15	0.04	0.04

TABLE VI

THE FITTING ERROR (IN PIXELS) OF THE COMPARED MODELS TO THE MATCHINGS BETWEEN A DIGITAL TEXTURED IMAGE AND ITS PHOTOGRAPH (WITH HOMOGRAPHY INITIALIZED BY 8-POINT ALGORITHM). THE MATCHINGS OBTAINED AT STEP 5 IN THE SUMMARIZED ALGORITHM ARE "OUTLIERS"-FREE AND PRECISE. COLUMN 1 IS THE ORDER OF THE MODEL. HALF OF THE MATCHINGS ARE USED TO ESTIMATE THE PARAMETERS AND THE AVERAGE FITTING ERROR SHOWN IS COMPUTED ON THE OTHER HALF BY APPLYING THE ESTIMATED PARAMETERS.

model	order	h_{11}	h_{12}	h_{13}	h_{21}	h_{22}	h_{23}	h_{31}	h_{32}	s
Radial	12	1.22	0.10	-170.16	0.015	1.24	-77.76	4.8×10^{-5}	1.1×10^{-4}	1.00
Division	12	1.22	0.10	-170.33	0.015	1.24	-77.49	4.8×10^{-5}	1.1×10^{-4}	1.00
FOV	12	1.22	0.10	-170.15	0.015	1.24	-77.76	4.8×10^{-5}	1.1×10^{-4}	1.01

TABLE V
THE ESTIMATED $\mathbf{H}$ AND $\mathbf{S}$ COMBINED WITH RADIAL SYMMETRIC MODELS OF ORDER 12 TO APPROXIMATE THE DISTORTION FIELD FROM DIGITAL PATTERN TO THE PHOTO.

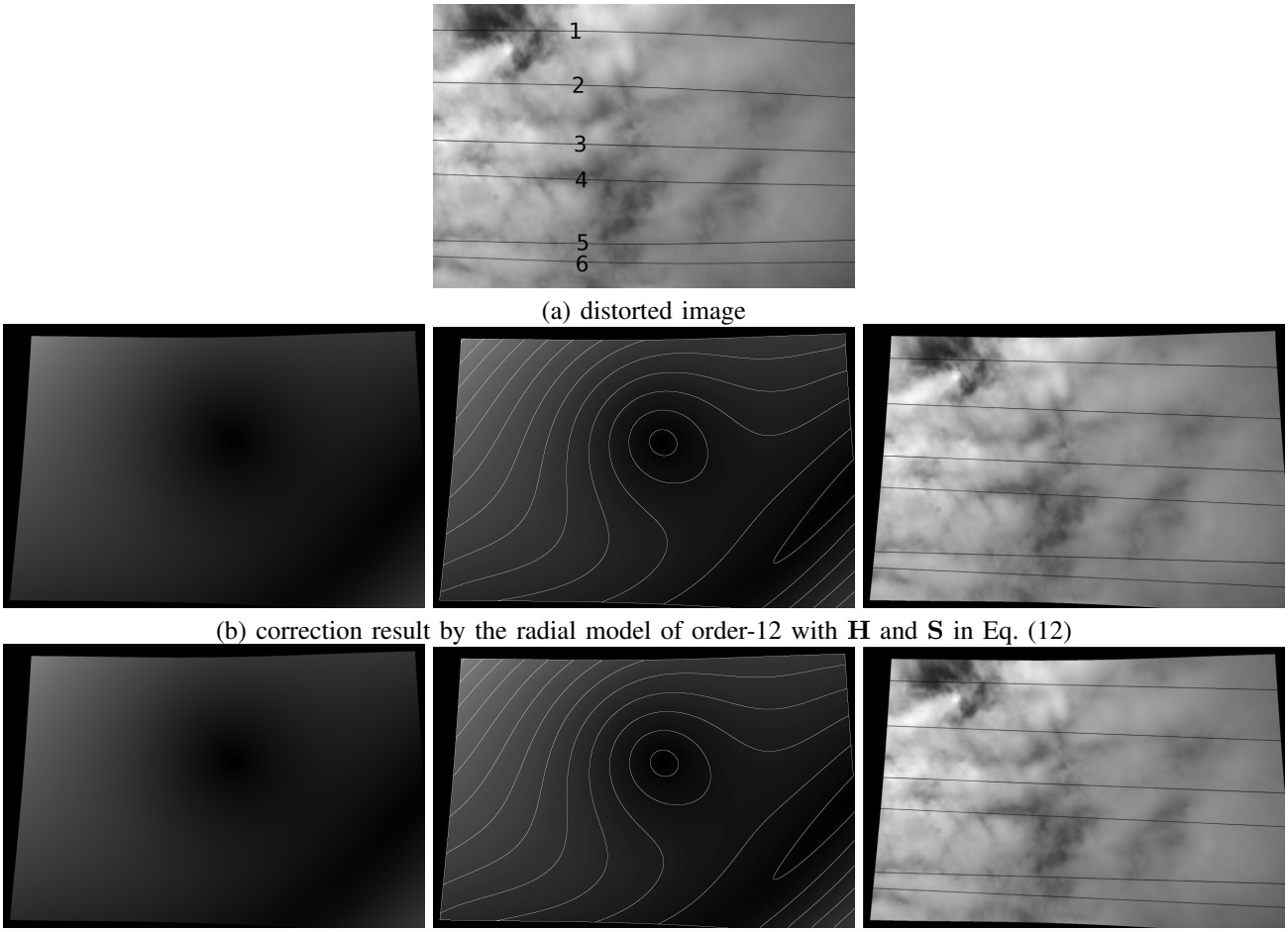

(a) distorted image

(b) correction result by the radial model of order-12 with $\mathbf{H}$ and $\mathbf{S}$ in Eq. (12)

(c) correction result by the polynomial model of order 12

Fig. 1. Top row: distorted image. Second row: the correction result by the radial model of order 12 with $\mathbf{H}$ and $\mathbf{S}$ in Eq. (12). Third row: the correction result by the polynomial model of order 12. From left to right column: the distortion field coded as the module of the displacement vector pointing from the digital pattern to the photo; the level line on the distortion field with quantification step of 10; corrected image. The results of the radial model and the polynomial model are visually identical. In fact, the results of all the tested parametric models are visually identical, according to the accuracy shown in Table VI and VII. The non-parametric method gives a slightly different result at the border due to the fact that the triangulation is imprecise at the border.

models are not capable to capture.

VI. CONCLUSION

We introduced the self-consistency and universality criteria for camera distortion models. Using these tools, five classic distortion models were evaluated and compared. The polynomial and rational model were shown to be both self-consistent and universal, to the cost of a high degree. This high degree raises no computational issue for the polynomial model. Indeed, we have seen that after a correct conditioning it can always be solved linearly (in contrast to the rational model). Furthermore, the polynomial model is translation invariant, which makes it insensitive to a translation of the distortion center. This model is not adapted to global camera calibration methods where the internal and external parameters and the distortion model are estimated simultaneously. The distortion correction must be dealt with as an independent and previous step to camera calibration. It might be objected that the high number of parameters in the polynomial interpolation (156 for an 11-order polynomial) could cause over-fitting bias in the results. This might be an objection when using over-simple calibration patterns. In our experiments the number of control points (about 4000) was far higher, about 30 times the number of polynomial coefficients. Our experiments show that the residual errors stabilize for orders between 6 to 12, confirming that no over-fitting occurred. Our experiments also show that

order	Radial	Division	FOV	Polynomial	Rational
3	0.27	0.27	0.27	0.74	0.11
4	0.19	0.21	0.19	0.58	0.09
5	0.19	0.21	0.19	0.15	0.09
6	0.19	0.21	0.19	0.09	0.09
7	0.19	0.21	0.19	0.09	0.09
8	0.19	0.21	0.19	0.09	0.09
9	0.19	0.21	0.19	0.09	0.09
10	0.19	0.21	0.19	0.09	0.09
11	0.19	0.21	0.19	0.09	0.09
12	0.19	0.21	0.19	0.09	0.09

TABLE VII
THE AVERAGED DISTANCE (IN PIXELS) FROM EDGE POINTS OF CORRECTED LINES TO THE CORRESPONDING REGRESSION LINE. THE PARAMETERS OF THE MODELS ARE ESTIMATED USING HALF OF THE MATCHINGS COMING FROM STEP 5 IN THE SUMMARIZED ALGORITHM. THE DISTORTED IMAGE IN FIG. 1 IS THEN CORRECTED BY USING ALL MODELS. THE CORRECTED LINES ARE EXTRACTED BY USING THE LINE SEGMENT DETECTOR IN [10], WHICH IS DESCRIBED IN DETAIL AND CAN BE TESTED ON LINE AT [11].

there is a small component of non radial symmetric distortion introduced by the camera, which cannot be modeled by radial symmetric models. High order polynomials are really needed to capture the non radial symmetric distortion if we wish to obtain high precisions. Clearly, this also entails two methodological changes: first that the distortion should be corrected independently and previously to projective calibration. Second, that calibration patterns should contain a higher than usual number of control points (more than 500). With the current image resolution in most cameras, this is no more a restriction.

REFERENCES

[1] L. Alvarez, L. Gomez, and J. Rafael Sendra. An algebraic approach to lens distortion by line rectification. *Journal of Mathematical Imaging and Vision*, 35(1):36–50, 2009.

[2] D.C. Brown. Close-range camera calibration. *Photogrammetric Engineering*, 37:855–866, 1971.

[3] M. Byrod, Z. Kukelova, K. Josephson, T. Pajdla, and K. Astrom. Fast and robust numerical solutions to minimal problems for cameras with radial distortion. *Computer Vision and Image Understanding*, 114(2):1–8, 2008.

[4] D. Claus and A. W. Fitzgibbon. A plumbline constraint for the rational function lens distortion model. *British Machine Vision Conference*, pages 99–108, 2005.

[5] D. Claus and A.W. Fitzgibbon. A rational function lens distortion model for general cameras. *IEEE Conference on Computer Vision and Pattern Recognition*, 1:213–219, 2005.

[6] F. Devernay. A non-maxima suppression method for edge detection with sub-pixel accuracy. Technical Report 2724, INRIA technical report, 1995.

[7] F. Devernay and O. Faugeras. Straight lines have to be straight. *Machine Vision and Applications*, 13:14–24, 2001.

[8] H. Farid and A. C. Popescu. Blind removal of lens distortion. *Journal of the Optical Society of America*, 18(9):2072–2078, 2001.

[9] A. W. Fitzgibbon. Simultaneous linear estimation of multiple view geometry and lens distortion. *IEEE Conference on Computer Vision and Pattern Recognition*, 1:125–132, 2001.

[10] R. Grompone von Gioi, J. Jakubowicz, J.M. Morel, and G. Randall. LSD: A fast Line Segment Detector with a false detection control. *IEEE Transactions on Pattern Analysis and Machine Intelligence*, 32(4):722–732, April 2010.

[11] R. Grompone von Gioi, J. Jakubowicz, J.M. Morel, and G. Randall. LSD: a Line Segment Detector. *Image Processing On Line*, 2012.

[12] R. Grompone von Gioi, P. Monasse, J.-M. Morel, and Z. Tang. Towards high-precision lens distortion correction. *IEEE International Conference on Image Processing*, pages 4237–4240, 2010.

[13] R. I. Hartley and T. Saxena. The cubic rational polynomial camera model. *Proc. DARPA Image Understanding Workshop*, pages 649–653, 1997.

[14] R.I Hartley and A. Zisserman. *Multiple View Geometry in Computer Vision*. Cambridge University Press, 2000.

[15] E. Kilpelä. Compensation of systematic errors of image and model coordinates. *Photogrammetria*, 37(1):15–44, 1980.

[16] Z. Kukelova and T. Pajdla. A minimal solution to the autocalibration of radial distortion. *IEEE Conference on Computer Vision and Pattern Recognition*, page 17, 2007.

[17] J. Lavest, M. Viala, and M. Dhome. Do we really need accurate calibration pattern to achieve a reliable camera calibration? *European Conference on Computer Vision*, 1:158–174, 1998.

[18] H. Li and R. Hartley. A non-iterative method for correcting lens distortion from nine point correspondences. *Workshop on Omnidirectional Vision (OMNIVIS)*, 2005.

[19] David G Lowe. Distinctive image features from scale-invariant keypoints. *International Journal of Computer Vision*, 60(2):91–110, 2004.

[20] Luis Gomez Luis Alvarez and J. Rafael Sendra. Algebraic lens distortion model estimation. *Image Processing On Line*, 2010.

[21] T. Pajdla, Z. Kukelova, and M. Bujnak. Automatic generator of minimal problem solvers. *European Conference on Computer Vision*, pages 302–315, 2008.

[22] T. Pajdla, T. Werner, and V. Hlavac. Correcting radial lens distortion without knowledge of 3-d structure. *Research Report, Czech Technical University*, 1997.

[23] B. Prescott and G. F. Mclean. Line-based correction of radial lens distortion. *Graphical Models and Image Processing*, 59:39–47, 1997.

[24] Gideon P. Stein. Lens distortion calibration using point correspondences. *IEEE Conference on Computer Vision and Pattern Recognition*, pages 602–608, 1997.

[25] D. Stevenson and M.M. Fleck. Nonparametric correction of distortion. Technical report, IEEE Workshop on Applications of Computer Vision (WACV), 1995.

[26] Z. Tang, R. Grompone von Gioi, P. Monasse, and J.M. Morel. High-precision camera distortion measurements with a "calibration harp". *Journal of the Optical Society of America A*, 29(10):2134–2143, 2012.

[27] M. Thirthala and S. Pollefeys. Multi-view geometry of 1d radial cameras and its application to omnidirectional camera calibration. *IEEE International Conference on Computer Vision*, pages 1539–1546, 2005.

[28] Roger Y. Tsai. A versatile camera calibration technique for high-accuracy 3d machine vision metrology using off-the-shelf tv cameras and lenses. *IEEE Journal of Robotics and Automation*, Vol. RA-3, 1987.

[29] J. Weng, P. Cohen, and M. Herniou. Camera calibration with distortion models and accuracy evaluation. *IEEE Transactions on Pattern Analysis and Machine Intelligence*, 14(10):965–980, 1992.

[30] Z. Zhang. On the epipolar geometry between two images with lens distortion. *International Conference on Pattern Recognition*, pages 407–411, 1996.

[31] Z. Zhang. A flexible new technique for camera calibration. *IEEE International Conference on Computer Vision*, pages 663–673, September 1999.